

Laser-Doppler Based Acoustic-to-Seismic Detection of Buried Mines

James M. Sabatier* and Ning Xiang

National Center for Physical Acoustics, University of Mississippi, MS 38677

ABSTRACT

Airborne acoustic waves coupled into the surface of the ground excite Biot Type I and II compressional and shear waves. This coupling of airborne sound into the ground is termed acoustic-to-seismic (A/S) coupling. If a land mine or other inhomogeneity is present below the surface, the ground surface vibrational velocity or S/A ratio will increase due to reflection and scattering of the Type II compressional wave. The dispersion characteristics of this wave in soils determines the mine detection limits. The S/A ratio is read with a Laser Doppler Vibrometer (LDV). The loud speaker and LDV were mounted onto a large forklift at Fort AP Hill. This system was used to scan patches of ground at the Fort AP Hill calibration mine lanes. An investigation on the variability of surface velocity over different background types and mine types is described. The results of these initial field exercises are described.

Keywords: Acoustic mine detection, acoustic-to-seismic coupling, Biot wave

1. INTRODUCTION

The concept of acoustic mine detection grew out of a research program whose focus was the coupling of airborne sound into the ground. We quickly learned that seismic sensors or geophones responded at higher levels than expected to the sounds of helicopters and other aircraft. This is due to the porous nature of the ground. Typically, the first few centimeters of the ground surface are 10-50% air by volume. This accounts for the enhanced coupling we observed. In subsequent research we were able to design probe microphones that could measure the pressure in the air-filled pores of the soil.

Assume that a "patch" of ground or roadway contains an AT mine buried a few centimeters below the surface. At the surface of the ground, the patch (typically a square meter) is insonified with a $10^2 - 10^4$ Hz frequency band at a 100 dB (re: 20 μ Pa) sound pressure level. This is easily accomplished with a vehicular mounted loudspeaker beamed towards the patch.

The sound source excites "Biot" Type II or slow speed vibrational waves in the porous soil. Because of the air present in the soil, this slow speed wave refracts toward the normal and propagates downward in the soil. If a mine or other inhomogeneity is present below the surface of the insonified patch, the transmitted slow wave is scattered or reflected by the target. For targets very close to the surface, the scattered field at the soil surface has the shape and size of the target. Taking advantage of a non-contact measurement technique, these surface vibrations are measured with a Laser Doppler Vibrometer (LDV).

The LDV is the heart of the system; it is state-of-the-art and capable of rapidly scanning the insonified path to read vibrational amplitudes. The LDV is mounted to the same platform as the acoustic source. As the laser beam is scanned across the insonified patch of ground, the light is Doppler shifted by the ground vibrational velocity. The reflected light from the ground now carries information that is optically detected and used to image buried targets. The collected light is mixed with the reference beam, demodulated, further filtered and Fourier transformed. The Fourier transformed signal at each pixel on the ground surface is processed in a manner to show the target.

In the following sections the physics of acoustic-to-seismic coupling is reviewed. In November 1998, acoustic-to-seismic coupling measurements were made at Fort AP Hill to demonstrate mine detection capabilities of S/A coupling measurement. The mine lanes at AP Hill are described. The background S/A signals in these lanes as well as the effects of buried mines on this measurement are presented. Comparisons of mine depth, type and soil condition on the detection capacity of S/A coupling are shown. For the forty buried mines scanned, the signal-to-noise ratio for on- and off-target signals is adequate to image the buried mine. These were not blind tests. The measurements showed little or no clutter. At this time the scanning rate is slow, but dramatic increases in scan rates are possible and appear to be limited by only the acoustic frequency.

* Correspondence: E-mail: sabatier@olemiss.edu, Ph. (601) 232-5404, Fax: (601) 232-7494

2. REVIEW OF ACOUSTIC-TO-SEISMIC COUPLING

In this section, the physics of sound propagation in soils is discussed. First, the Biot¹ poro-elastic description of soils is presented. Second, the main features of this model and measurements as related to acoustic detection of mines are discussed.

When airborne sound is incident on the surface of a soil,²⁻⁴ air contained by connected pores in the soil is caused to oscillate in and out of the pores. The resulting area-average volume flow is governed both by the frequency and amplitude of the sound waves and by the properties of the soil. The energy from the vibrating air above the soil surface couples with the air in the soil pores. Hence, the penetration of the sound waves is strong if the air permeability is high. The transmitted sound is attenuated by viscous friction present at the pore walls. Conversely, low air permeability means weak coupling and little sound penetration. Through momentum transfer at the air-soil boundary and viscous attenuation at the pore walls, the energy is transferred to the soil matrix. Strictly speaking, this transfer of energy to the fluid-filled soil must be treated by a poro-elastic wave theory. One model used to successfully describe this coupling is that of Biot.¹

The Biot¹ equations of motion admit two compressional wave solutions and thus two propagation constants or wave speeds. The waves are referred to as the waves of the first and second kinds or simply as fast and slow waves. Both of these waves propagate simultaneously in both fluid and solid so that for each wave there is both fluid and solid displacement. The slow wave is a diffusion wave that is highly attenuated and very dispersive as it propagates. The fast wave is analogous to the compressional or seismic p wave that propagates in a solid. It is relatively unattenuated and not dispersive.

In Figs. 1 and 2, the ratios of the solid to fluid displacement amplitude for the fast and slow wave for typical soil properties is shown.

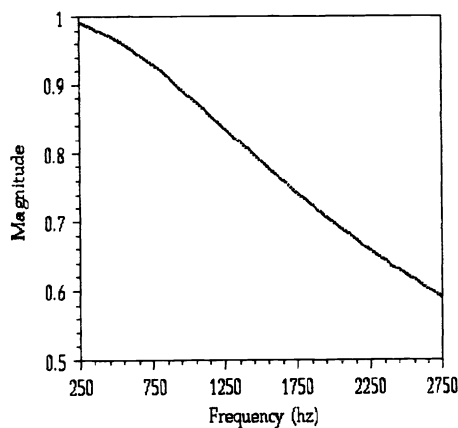


Figure 1. Ratio of solid to fluid displacement for the fast wave.

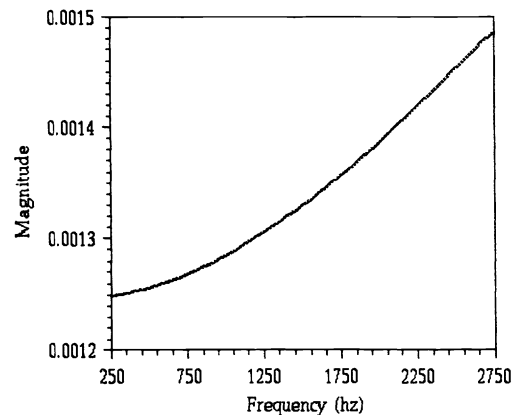


Figure 2. Ratio of solid to fluid displacement for the slow wave.

These results show that in the frequency range of interest and, for the slow wave, most of the energy is found in the fluid displacement. Note in Fig. 2 that the ratio is much less than one. For the fast wave, most of the energy is in matrix displacement. This is the reason it is often assumed that the slow wave is only an acoustic wave propagating in the pore space and the fast wave is a seismic wave propagating in the soil matrix. With this in mind, one would expect a geophone or matrix sensor to respond to fast waves and a buried microphone to respond to slow waves. This is the case, but in well controlled, low noise experiments both wave types can be observed with each sensor.⁵ Similar calculations yield phase velocity and attenuation of each wave type. These results are shown in Figs. 3 and 4. The fast wave shows no dispersion (constant speed of 260m/s) and relative to the slow wave very little attenuation. Comparatively, slow wave speed is rather slow, but very dispersive. This very slow and highly attenuated wave is quite surprising. Its characteristics in soils have been well documented.

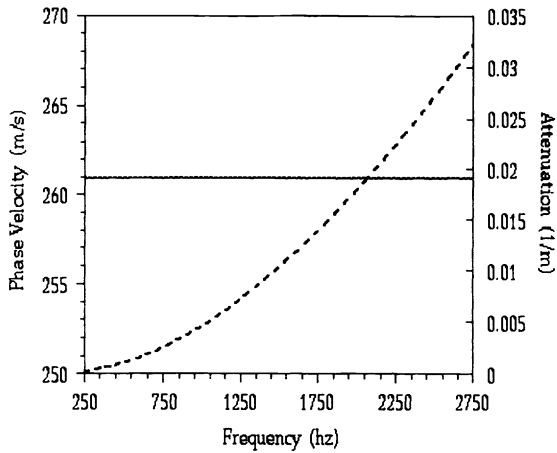


Figure 3. Velocity (solid line) and attenuation for fast wave.

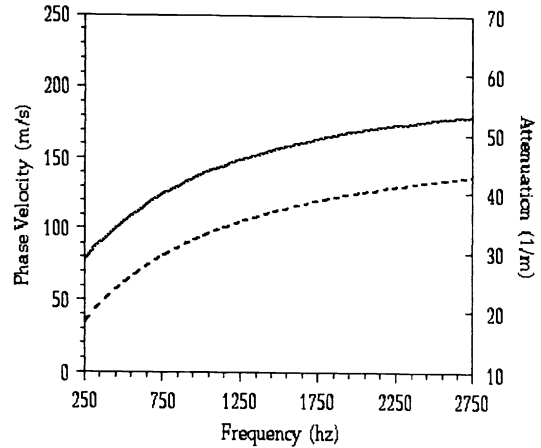


Figure 4. Velocity (solid line) and attenuation for slow wave.

In Fig. 5, the pressure for sand material and a loess soil, as measured by a buried microphone due to an air-borne sound source, is shown as a function of depth below the soil surface. Each figure shows two distinct slopes. Because the source of sound is mechanically de-coupled from the soil surface, the energy is preferentially transmitted to the slow wave at the boundary. This is because the impedance of the air in the soil pores is much less than that of the soil matrix. Since the slow wave is rapidly damped with distance, the microphone at deeper depths is responding to the fast wave pressure. Velocity data showing the same effect have been produced using geophones as receivers. In Fig. 6, velocity measurements using buried microphones, probe microphones and geophones are shown for a suspended loud speaker. These data show two velocities, detected on both sensors. The “transition depth” (between 10-20cm) in Fig. 6 corresponds to the depth where both wave types are of approximately the same amplitudes. At or below this depth the slow wave cannot be detected.

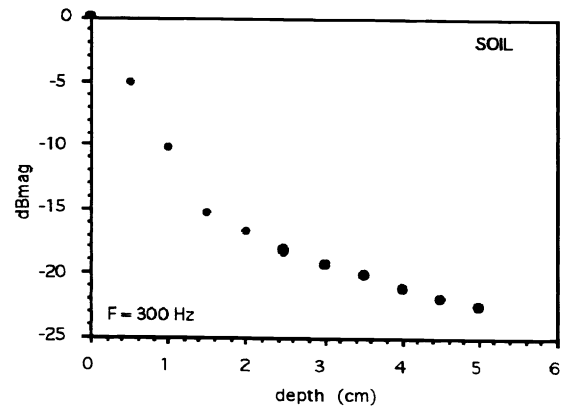
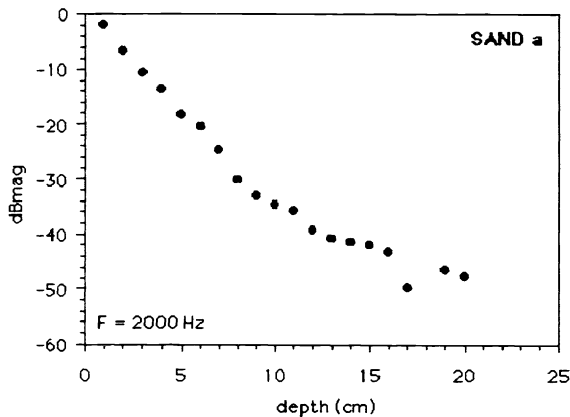


Figure 5a,b. Pressure measured with a buried microphone shows attenuation coefficients for fast and slow waves.

The important results of this review of the physics of air-filled soils are as follows. Air-borne sound is preferentially coupled into the soil as slow wave energy. The speed of this wave is much slower than the sound speed in air, so the slow wave is locally reacting or refracted towards the normal. The slow wave dilates both the air and soil matrix as it propagates. Therefore, slow wave effects can be detected by sensing the matrix or the gas. The attenuation of the slow wave is well modeled and it is rapidly dampened with depth. Detection depth will be controlled by the slow wave attenuation coefficient. The wavelength of the slow wave and the sensing area of the sensor will control target resolution. From the above, an understanding is provided of the physics on how buried, non-porous inhomogeneities are acoustically detected in soils.

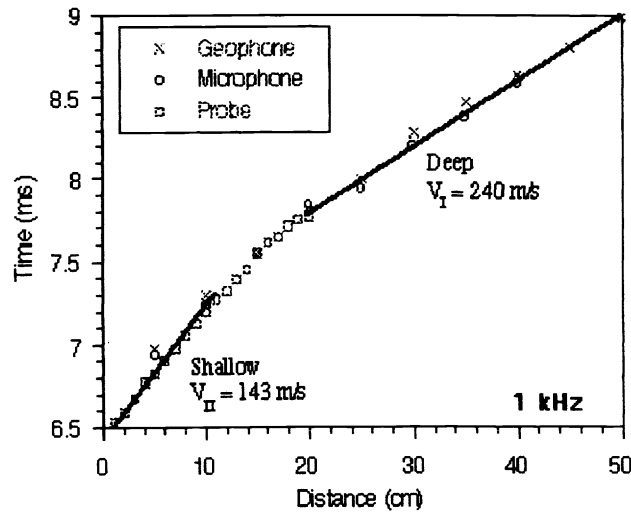


Figure 6. Times of arrival of pulses as a function of depth for three sensors, probe microphone, buried microphone and geophone, showing velocity of the fast wave (deep) and slow waves (shallow).

3. AP HILL SITE DESCRIPTION

Acoustic-to-Seismic coupling measurements were made lanes 13, 14 and 16 at AP Hill. Lane 13, locally referred to as a “dirt road,” is a composite gravel and sandy clay mixture. The gravel size is nominally 0.02m. Sand/clay grain sizes were approximately 10-100 microns. The density of the gravel in this site is about as high as possible. Although there was no gravel on the surface, a pocketknife could not be pushed into the road surface more than a centimeter at any point on the surface of this lane. Lane 14 is referred to as the gravel road. This lane is a composite of broken granite rock and a crushed granite binder. The nominal size of the granite rock was 0.02m. The crushed granite binder was much larger than that used in the clay gravel road. Crushed granite grain sizes were approximately 10-1000 microns. Lane 14, as opposed to Lane 13, had a single layer of granite rock on the surface. After removing this surface rock layer, the granite rock density was such that a pocketknife could not be pushed deeper than a centimeter into the surface. Lane 16 is referred to as the “off-road” site. This lane is composed of the local soil at AP Hill. It is a fine grain sandy loam. The soil was free of rocks and homogeneous compared to lane 13 and 14. Grass grows on the surface to a height of 0.1-0.15m and is sparsely covered with leaves from near by hardwood trees. No attempts were made to remove leaves from the surface prior to measurements.

4. BACKGROUND VELOCITY VARIABILITY

In this section, the measured acoustic-to-seismic coupled background velocity variability for one of the three road surfaces is presented. The ground surfaces studied included a clay-gravel road (“dirt road”), a granite-gravel road and an off-road site. Figure 7 shows five individual magnitude spectra of the background velocity at co-ordinates X = 1.796 m and Y = 6.085 m of lane 13. These five measurements occur within an area of 1 m². The loudspeaker voice coil current is 0.6A and the signal bandwidth is 60-280Hz. Two strong peaks can be found below 120 Hz. Previous experimental measurements have shown that such low frequency peaks are S/A resonances and are associated with ground layering on the order of a few meters. Additionally, a much broader peak occurs above 220 Hz. Resonances in this frequency range are typically associated with a ground layers within the first meter of the surface. This broad peak is associated with the man-made roadbed layer depth of this lane. These same peaks are observed in other measurements on this lane.

Averaged magnitude spectra measured at five locations down the length of the lane (Y coordinate from 3 m to 15 m) are depicted in Fig. 8. Here the frequency span is reduced (80-250Hz) and the voice coil current increased from 0.6 to 1.0A. As a result of the higher sound pressure levels at the measurement points, the background velocity is increased. The variability in the background velocity over this much larger area is no greater than any other location on this lane. Another common feature of all of these background velocity spectra is the lack of resonant structure between 100 and 200Hz. Similar analysis of the other two lanes shows the same lack of variability in the background velocity.

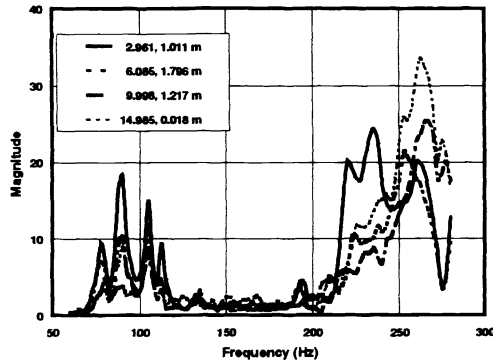


Figure 7. S/A velocity ($\mu\text{m/s}$) variability on clay-gravel road.

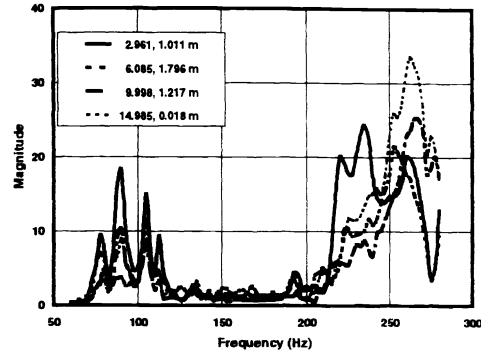


Figure 8. S/A velocity ($\mu\text{m/s}$) variability on clay-gravel road.

5. TARGET SIGNATURES

The magnitude of the acoustically coupled velocity depends upon the magnitude of the acoustic pressure. In Fig. 9, the effect of increasing the voice coil current to the loudspeaker on the magnitude of the surface particle velocity is shown. The solid line and short dash line are the on-target velocity magnitude for voice coil currents of 1.0A and 0.6A. The long dash line is the 0.6A off-target velocity ($\mu\text{m/s}$) amplitude. The target is an M15 at a 6 inch depth in lane 13. Clearly increasing the sound pressure increases both the on- and off-target velocity. In the measurements taken at AP Hill mine lanes, the sound pressure level from site to site varied. Initially, low acoustic levels were broadcast, but as the measurement exercise proceeded, higher SPL's were needed to detect deeper mines. This was accomplished by decreasing the acoustic bandwidth and increasing the loudspeaker voice coil current.

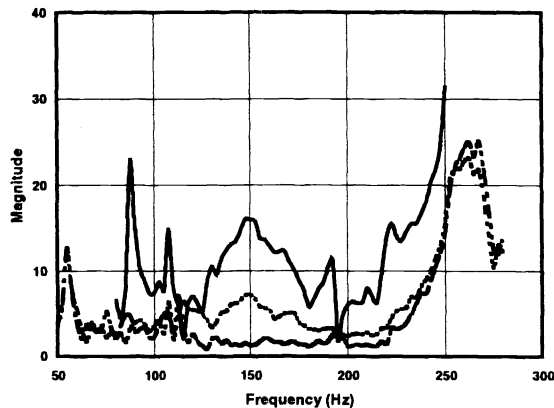


Figure 9. Effect of increased voice coil current on S/A ratio.

Averaged off-target and on-target velocity frequency responses are described above to demonstrate signal/noise ratios. To remove the variable site-to-site SPL, the following calculation was done. Since both the S/A background velocity and S/A on-target velocity are produced with the same acoustic signal, one can consider the ratio or transfer function of the on- and off-target velocity. Further, since the wavelength of the sound used to drive the ground is typically 3.5m and the typical scan area is less than a meter, the pressure over the scan area can be assumed to be uniform. Therefore, the influence of the sound source bandwidth and voice coil current can be removed by computing on-target/off-target ratio.

The spatial seismic/acoustic transfer function is defined as the ratio of the magnitudes of the spatially averaged velocity frequency response on the target to the spatially averaged background velocity frequency response. If values of this transfer function are less than one, the on-target velocity is smaller than the background velocity at that particular frequency. Since the voice coil current and frequency bandwidth of the source signal are varied considerably in the measurements, this transfer function provides a means of removing this variance. Fine structure due to small variability in the off-target velocity is introduced in this spatially normalized on-target velocity-ratio frequency response. To demonstrate the magnitude of this effect,

the ratio of the off-target velocity frequency response at nearby locations is calculated. In Fig. 10, the five-point average on-target velocity frequency response, the ratio of two five-point off-target velocity frequency responses and the ratio of the on-target frequency response and one of the off-target responses (not shown) are shown for a VS2.2 at one inch in lane 13. Ideally this transfer function for nearby locations should be one for all frequencies. The deviations from one are due to local variations in the off-target velocity or background A/S coupling. This normalization scheme allows for comparisons of the on-target signatures of mines at different depths and lanes as well as mine type even though the SPL varied from site to site.

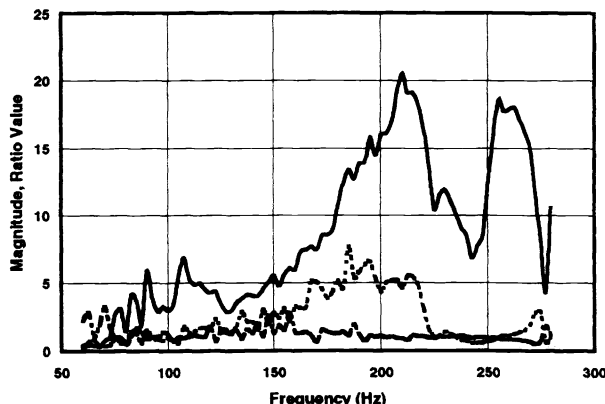


Figure 10.

Table 1 lists the AT mines that were scanned in the calibration lanes at AP Hill. Referring to Table 1, the data collected allows for comparisons of the same mine type and mine depth at two locations in the same lane for only one case, the M15 mine in lane 15. Referring again to this table, comparisons of the mine type at various depths in the same lane can be made. For example, a VS2.2 at one and four inches in lane 14 can be compared.

Table 1. AT Mines Scanned at AP Hill								
Lane ID Number	Anti-Tank Landmines (Mine Depth in Inches)							
	M15	M19	M21	TMA4	TM62M	TM62P	VS1.6	VS2.2
13	3	5	1	2	6	2	1, 6	1
14	3, 6		2	6		3	4	1, 4
16		3						3

Figure 11 shows the normalized on-target signature ratio of an M15 at one inch in the off-road lane at two locations. The main feature of this data is the similarity of the two signatures. Figure 12(a, b, c) shows the effect of depth for three different mines. Figure 12a shows the normalized velocity ratio for a VS1.6 at depths of one and six inches in lane 15, the off road site. Figure 12b shows similar data for an M15 at depths of three and six inches in lane 14m, the granite gravel road. Figure 12c shows data for a VS2.2 at depths of one and four inches in lane 14. All these data show that the magnitude of the velocity of the ground surface decreases with the depth of the target. Further, one can observe that this attenuation increases with frequency.

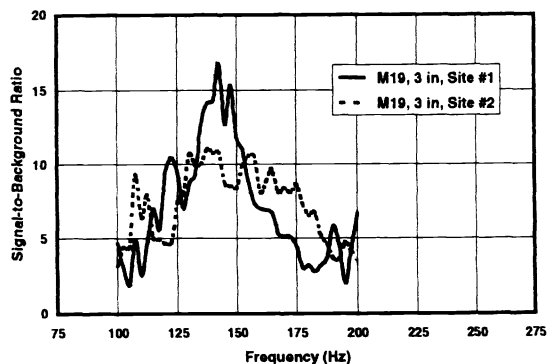


Figure 11. Signature of M15 at two locations in off-road site.

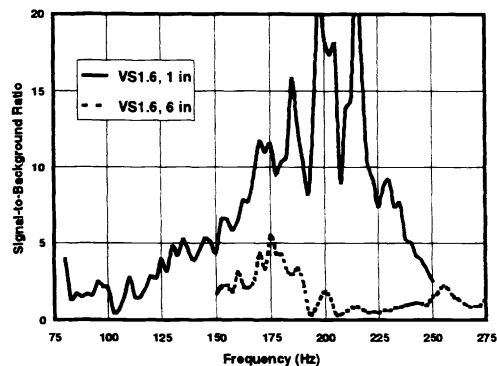


Figure 12a. Target depth effect, VS1.6 in off-road site.

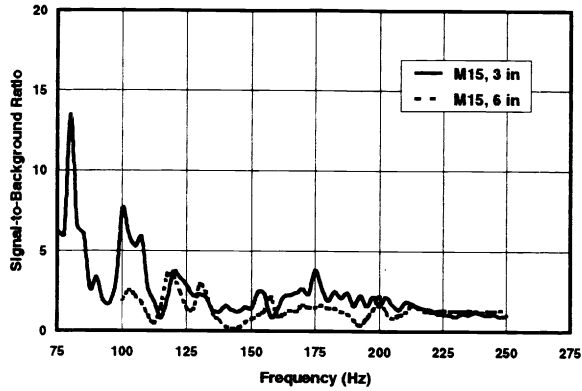


Figure 12b. Target depth effect, M15 in granite gravel road.

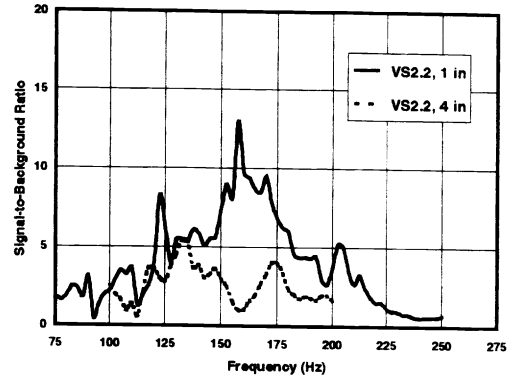


Figure 12c. Target depth effect, VS2.2 in granite gravel road.

The LDV has capabilities to make a raster scan. In Fig. 13 the RMS velocity at 230Hz is plotted at each of 256 pixels of such a scan. The pixel spacing is approximately 0.07m and the scan area 1m². The acoustic wavelength driving the surface of the ground is 1.5m, therefore the imaged area is moving in phase. The presence of the mine distorts the surface particle velocity in the vicinity of the mine. The spatial distribution of the surface velocity appears as modes of a circular membrane. Although it is not shown the phase of the velocity over the mine is $\pi/2$ out of phase from the background velocity. This result is well known for the rigid-backed porous material impedance. Although a single point measurement can be made in a few milliseconds, this velocity map of the soil takes 1/3 hour to complete. This long scan time is currently a software limit.

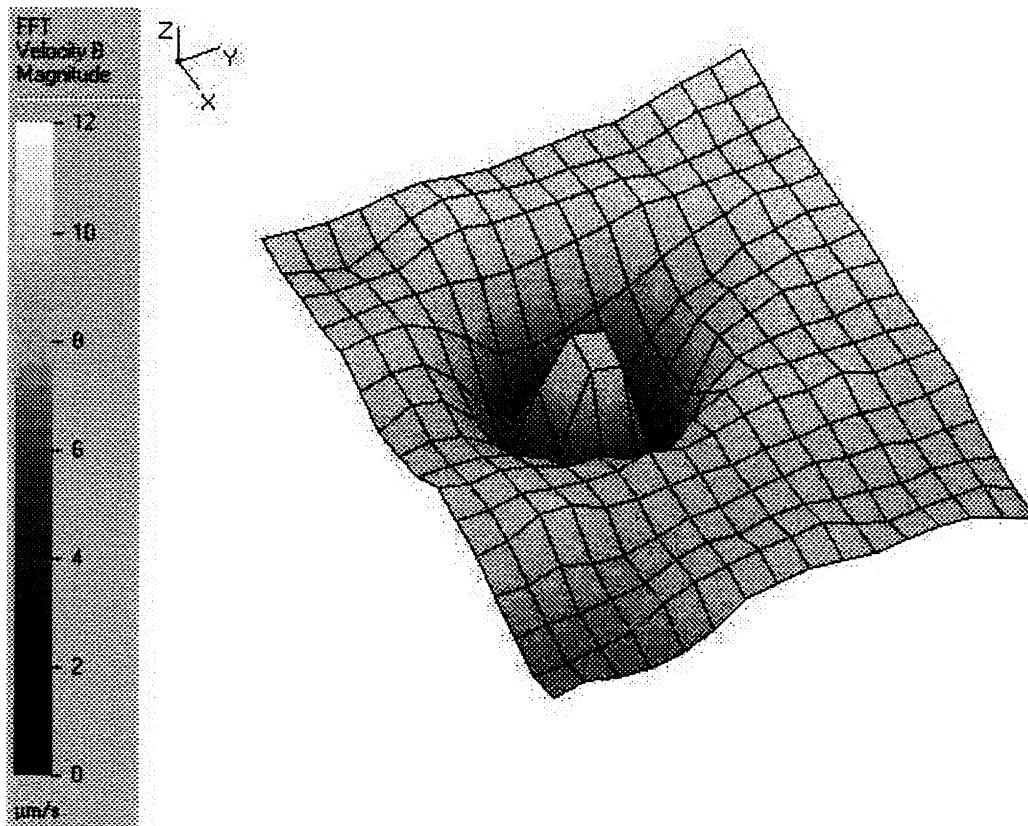


Figure 13. S/A frequency response at 230 Hz for a VS1.6 at 1 in. in clay gravel road.

6. CONCLUSIONS

At the recent AP Hill exercises, the A/S coupling mine detection technique has been able to detect 100% of the mines in the lanes that were scanned. These initial field exercises have shown little or no clutter. The positional accuracy of the technique is on the order of an inch. However, these were not blind tests. Normal incidence standoff distances of 1-3m were successfully used in these exercises.

The Biot slow wave that propagates in a poro-elastic material is sensitive to the soil porosity, flow resistivity and tortuosity. The fact that man-made plastic and metallic mines are non-porous allows for a sharp contrast in the acoustic impedance that the slow wave senses. Further research will increase scan rates and build additional data bases of mine types, depth and soil types.

7. ACKNOWLEDGEMENTS

This work is supported by the U S Army Communications-Electronics Command, Night Vision Laboratory.

REFERENCES

1. Biot, M. A., "Theory of propagation of elastic waves in a fluid saturated porous solid. II higher frequency range," J. Acoust. Soc. Am. 28, 179-91 (1956).
2. Sabatier, J.M., Bass, H.E., Bolen, L.N., Attenborough, K. and Sastry, V.V.S.S., "The interaction of airborne sound with the porous ground: The theoretical formulation," J. Acoust. Soc. Am. 79, 1345-52 (1986).
3. Sabatier, J.M., Bass, H.E., Bolen, L.N. and Attenborough, K., "Acoustically induced seismic waves," J. Acoust. Soc. Am. 80, 646-9 (1986).
4. Attenborough, K., Sabatier, J.M., Bass, H.E. and Bolen, L.N., "The acoustic transfer function at the surface of a layered poro-elastic soil," J. Acoustic. Soc. Am. 79, 1353-8 (1986).
5. Hickey, C.J. and Sabatier, J.M., "Measurements of two types of dilatational waves in an air-filled unconsolidated sand," Accepted to J. Acoust. Soc. Am. 2/5/97.